The origin and underlying driving forces of the SARS-CoV-2 outbreak

Shu-Miaw Chaw[1¶], Jui-Hung Tai[1,2], Shi-Lun Chen[3], Chia-Hung Hsieh[4], Sui-Yuan Chang[5], Shiou-Hwei Yeh[6], Wei-Shiung Yang[2], Pei-Jer Chen[2], and Hurng-Yi Wang[2,7, ¶*]

[1] Biodiversity Research Center, Academia Sinica, Taipei, Taiwan

[2] Graduate Institute of Clinical Medicine, College of Medicine, National Taiwan University, Taipei, Taiwan

[3] Department of Life Science, National Taiwan Normal University, Taipei, Taiwan

[4] Department of Forestry and Nature Conservation, Chinese Culture University, Taipei, Taiwan

[5] Department of Microbiology, College of Medicine, National Taiwan University, Taipei, Taiwan

[6] Department of Clinical Laboratory Sciences and Medical Biotechnology, College of Medicine, National Taiwan University, Taipei, Taiwan

[7] Institute of Ecology and Evolutionary Biology, National Taiwan University, Taipei, Taiwan

Corresponding Author

E-mail: hurngyi@ntu.edu.tw (HYW)

[¶]These authors contributed equally to this work

Running Title: Evolution at the early stage of SARS-CoV-2 spread

Keywords: positive selection, population genetics, coronavirus, mutational bias,

Abstract

The spread of SARS-CoV-2 since December 2019 has become a pandemic and impacted many aspects of human society. Here, we analyzed genetic variation of SARS-CoV-2 and its related coronavirus and found the evidence of intergenomic recombination. After correction for mutational bias, analysis of 137 SARS-CoV-2 genomes as of 2/23/2020 revealed the excess of low frequency mutations on both synonymous and nonsynonymous sites which is consistent with recent origin of the virus. In contrast to adaptive evolution previously reported for SARS-CoV in its brief epidemic in 2003, our analysis of SARS-CoV-2 genomes shows signs of relaxation of selection. The sequence similarity of the spike receptor binding domain between SARS-CoV-2 and a sequence from pangolin is probably due to an ancient intergenomic introgression. Therefore, SARS-CoV-2 might have cryptically circulated within humans for years before being recently noticed. Data from the early outbreak and hospital archives are needed to trace its evolutionary path and reveal critical steps required for effective spreading. Two mutations, 84S in orf8 protein and 251V in orf3 protein, occurred coincidentally with human intervention. The 84S first appeared on 1/5/2020 and reached a plateau around 1/23/2020, the lockdown of Wuhan. 251V emerged on 1/21/2020 and rapidly increased its frequency. Thus, the roles of these mutations on infectivity need to be elucidated. Genetic diversity of SARS-CoV-2 collected from China was two time higher than those derived from the rest of the world. In addition, in network analysis, haplotypes collected from Wuhan city were at interior and have more mutational connections, both of which are consistent with the observation that the outbreak of cov-19 was originated from China.

SUMMARY

In contrast to adaptive evolution previously reported for SARS-CoV in its brief epidemic, our analysis of SARS-CoV-2 genomes shows signs of relaxation of selection. The sequence similarity of the spike receptor binding domain between SARS-CoV-2 and a sequence from pangolin is probably due to an ancient intergenomic introgression. Therefore, SARS-CoV-2 might have cryptically circulated within humans for years before being recently noticed. Data from the early outbreak and hospital archives are needed to trace its evolutionary path and reveal critical steps required for effective spreading. Two mutations, 84S in orf8 protein and 251V in orf3 protein, occurred coincidentally with human intervention. The 84S first appeared on 1/5/2020 and reached a plateau around 1/23/2020, the lockdown of Wuhan. 251V emerged on 1/21/2020 and rapidly increased its frequency. Thus, the roles of these mutations on infectivity need to be elucidated.

INTRODUCTION

A newly emerging coronavirus was detected in patients during an outbreak of respiratory illnesses starting in mid-December of 2019 in Wuhan, the capital of Hubei Province, China [1 , 2, 3]. Due to the similarity of its symptoms to those induced by the severe acute respiratory syndrome (SARS) and genome organization similarity, the causal virus was named SARS-CoV-2 by the International Committee on Taxonomy of Viruses [4]. As of 3/16/2020, 167,515 cases of SARS-CoV-2 infection have been confirmed in 114 countries, causing 6,606 fatalities. As a result, WHO declared the first pandemic caused by a coronavirus on 3/11/2020 (https://www.who.int/emergencies/diseases/novel-coronavirus-2019/situation-reports). As the virus continues to spread, numerous strains have been isolated and sequenced. On 3/18/2020, more than 500 complete or nearly complete genomes have been sequenced and made publicly available.

SARS-CoV-2 is the seventh coronavirus found to infect humans. Among the other six, SARS-CoV and MERS-CoV can cause severe respiratory illness, whereas 229E, HKU1, NL63, and OC43 produce mild symptoms [5]. Current evidence strongly suggests that all human associated coronaviruses originated from other animals, such as bats and rodents [5, 6]. While SARS-CoV-2 shares similar genomic structure with other coronaviruses [7-10], its sequence differs substantially from some of the betacoronaviruses that infect humans, such as SARS-CoV (approximately 76% identity), MERS-CoV (43% identity), and HKU-1 (33% identity), but exhibits 96% similarity to a coronavirus collected in Yunnan Province, China from a bat, *Rhinolophus affinis*. Therefore, SARS-CoV-2 most likely originated from bats [2, 11].

Several issues concerning the origin, time of virus introduction to humans, evolutionary patterns, and the underlying driving force of the SARS-CoV-2 outbreak remain

to be clarified [12, 13]. Here, we analyzed genetic variation of SARS-CoV-2 and its related coronaviruses. We discuss how mutational bias influences genetic diversity of the virus and attempt to infer forces that shape SARS-CoV-2 evolution.

RESULTS

Molecular evolution of SARS-COV-2 and related coronaviruses

The resulting phylogeny reveals that RaTG13 is the closest relative of SARS-COV-2, followed by pangolin_2019 and pangolin_2017, then CoVZC45 and CoVZXC21, and other SARS-related sequences as outgroups (S1 Fig). According to general time reversible model, transition occurred more frequent than transversion with C-T and A-G changes account for 45% and 28%, respectively, of all six types of nucleotide changes. We next estimated the strength of selection for each coding region using the dN and dS. While purifying selection tends to remove amino acid-altering mutations, thus reducing dN and dN/dS, positive selection has the opposite effect, increasing dN and dN/dS [14]. Between SARS-CoV-2 and RaTG13, *orf8* gene exhibits the highest dN (0.032) followed by *spike* (0.013) and *orf7* (0.011), all above the genome average of 0.007 (Table 1). dS varies greatly among CDSs with the highest of 0.313 in *spike* and the lowest of 0.018 in *envelope* (genome average 0.168). Finally, dN/dS is the highest in *orf8* (0.105) followed by *orf7* (0.061) and *orf3* (0.060), with the genome average of 0.042. Since *spike* shows both high dS and dN, its protein evolution rate (dN/dS) is only 0.040. Thus, while the coronavirus evolved very rapidly, it has actually been under tremendous selective constraint [13].

Spike protein similarity between SARS-CoV-2 and pangolin_2019 led to the idea that the receptor binding domain (RBD) within the SARS-CoV-2 spike protein originated from pangolin_2019 via recombination [15-18]. If that were the case, we would expect the divergence at synonymous sites (dS) to also be reduced in the RBD region. However, while

dN in the RBD region is 0.023, approximately one third of the estimate for the rest of the *spike* gene (0.068), dS in the RBD (0.710) is actually slightly higher than in the rest of the *spike* sequence (0.651). This argues against the recombination scenario. We noticed that the dS of the whole *spike* and the RBD, are 2- and 3-fold, respectively, higher than the genome average. Since synonymous sites are typically less influenced by selection, the increased divergence in dS may reflect an underlying elevated mutation rate.

Genetic variation of SARS-CoV-2

We downloaded 137 SARS-CoV-2 genomes available from GISAID as of 2/23/2019. The coding regions were aligned and 223 mutations were identified with 68 synonymous and 115 nonsynonymous changes. The directionality of changes was inferred based on the RaTG13 sequence. Frequency spectra of both synonymous and nonsynonymous changes are skewed. While the former shows excess of both high and low frequency mutations, the latter mainly exhibits an excess of low frequency changes (Fig. 1a). The excess of low frequency mutations is consistent with the recent origin of SARS-CoV-2 [19]. Both population reduction and positive selection can increase high frequency mutations [20, 21]. However, the first scenario is contradicted by the recent origin of the virus. If positive selection has been operating, we would expect an excess of high frequency non-synonymous as well as synonymous changes. Furthermore, the ratio of nonsynonymous to synonymous changes is 2.46 (138/56) among singleton variants, but only 1.42 (17/12) among non-singletons. Both of these observations suggest that the majority of amino acid-altering mutations are selected against, with no positive selection in evidence.

The skew of synonymous variants toward high frequency deserves further discussion, as it relates to the underlying force driving the SARS-CoV-2 outbreak. The puzzle is probably rooted in how high and low frequency mutations are inferred. The results shown in

the Fig. 1a are based on an outgroup comparison. The divergence at synonymous sites between SARS-CoV-2 and RaTG13 is 17%, approximately 3-fold greater than between humans and rhesus macaques [22]. With such high level of divergence, the possibility of multiple substitutions cannot be ignored, especially since substitution in the coronavirus genome is strongly biased toward transitions (see above). Indeed, among all non-singleton mutations listed in Table 2, 62% of the changes are C-T transitions.

To get around the potential problem caused by multiple substitutions, we cross-referenced the course of changes using the SARS-CoV-2 haplotype network (Fig. 2) and phylogeny (S2 Fig). The two analyses yield very different pictures. For example, the highest frequency derived mutation in Table 2 is a C-T synonymous change at 10138 (marked γ in Fig 2 and Table 2). All three sequences from Singapore share the T nucleotide also found in the RaTG13 outgroup. Using the outgroup comparison, the C found in the rest of the human SARS-CoV-2 sequences is a derived mutation. However, the T at this position is restricted to genomes collected from Singapore on 2/4 and 2/6/2020 and not found in earlier samples. It is thus more sensible to infer that this T is a back mutation derived from C rather than an ancestral nucleotide. Another synonymous change at position 24034 occurred twice (C24034T) on different genomic backgrounds (marked κ in Fig 2). Although the outgroup sequence at this position is T, it is more likely that the C at this position is the ancestral nucleotide. We observed a number of such back or repeated mutations. An A-T nonsynonymous change at 29019 (D249H in nucleocapsid protein, marked O in Fig. 2) also occurred twice.

Repeated mutations may be caused by intergenomic recombination. Indeed, the result of four haplotype test suggested that at least two recombination events may have occurred between positions 8782 and 11083 and between 11083 and 28854. We noticed that a sequence isolated on 1/21/2020 from a patient in the United States (EPI_ISL_404253)

exhibited Y (C or T) at both positions 8,782 and 28,144. Although, the possibility that two novel mutations might be occurred within this patient cannot be 100% ruled out, the alternative explanation that this patient may have been co-infected by two viral strains seems more plausible.

After cross-referencing with the haplotype network and the phylogeny, all mutations listed as high frequency in Table 2 and Fig. 1a were re-assigned to the other side of the frequency spectra. We only see an excess of singleton mutations, consistent with a recent origin of SARS-CoV-2 (Fig. 1b) and suggesting that the virus has mainly evolved under constraint.

Perhaps the most controversial case is the T-C change at position 28814 which alters Leucine (L) to Serine (S) in orf8 protein (L84S). Since both pangolin and RaTG13 have a C at this position (Table 2), Tang et al suggested that 84L is derived from 84S in the human virus [13]. The 84S was not discovered until 1/5/2020, by which time 23 SARS-CoV-2 genomes have been sampled. After the first appearance, its frequency gradually increased, reaching approximately 30% by 1/23/2020, suggesting that 84S may exhibit some advantage over 84L. If genomes carrying 84S were ancestral, it would be a challenge to explain its absence in early samplings. In addition, as mentioned above, C-T transitions are dominant in coronavirus evolution and multiple hits were observed in SARS-CoV-2 (Fig. 2). It is therefore possible that 28814C mutated to T after ancestral SARS-CoV-2 diverged from the common ancestor with RaTG13 and recently changed back to C. Finally, if 84L is indeed a derived haplotype and has rapidly increased in its frequency by positive selection, we would expect haplotypes carrying 84L to have accumulated more derived mutations than haplotypes with 84S. However, after correcting for mutational direction, the two haplotypes exhibited similar mutation frequency spectra (S3 Fig). The alternative hypothesis that 84S is a back mutation from 84L is more plausible.

Selection pressure on SARS-CoV-2

In addition to L84S, a G-T transversion at 26114 which caused an amino acid change in orf3 protein (G251V) is also at intermediate frequency (Table 2). 251V was first seen on 1/22/2020 and gradually increased its frequency to 13% by our sampling date (Fig. 3). We note that the emergence of 84S in orf8 and 251V in orf3 are consistent with the lockdown of Wuhan on 1/23/2020. The former first appeared in early January, gradually increased its frequency, and reached a plateau around 1/23/2020. The latter showed up on 1/22/2020 and rapidly increased its frequency within two weeks.

Based on Fig. 3, we divided the sampling course into two epidemic episodes, from the first sampled sequence (12/24/2019) to before the lockdown of Wuhan (1/21/2020) and from 1/22/2020 to the date of the last sequence sampling (2/23/2020). The dN/dS of coding regions within the two episodes were estimated. As roughly 87% of mutations were singletons. Many of these are probably sequencing errors, affecting synonymous and nonsynonymous sites equally and inflating our dN/dS estimates. In addition, since dN/dS is already extremely small in SARS-CoV-2 (Table 1), such inflation would have a large effect on dN/dS estimates. We therefore excluded singletons from dN and dS estimation.

The dN/dS of *orf8* gene in episode I and II and *orf3* gene in episode II show strong signatures of positive selection, consistent with increase of 84S and 251V frequency during these periods, and may suggest a role of adaptation (Table 3). The overall dN/dS within each episode was 5-10 times higher than dN/dS between coronavirus genomes derived from different species (Table 1). The elevated dN/dS of SARS-CoV-2 is either due to its adaptation to human hosts or relaxation of selection. For a recently emerged virus, it is reasonable to expect operation of positive selection at the early stage. In that case, the dN/dS during episode I should be greater than during episode II [23, 24].

However, dN/dS was smaller in episode I than in episode II across the majority of the genome, suggesting that elevation of dN/dS is probably mostly due to the relaxation of selection. We further divided episode I into Ia and Ib, according to the appearance of 84S in orf8 protein on 1/6/2020. The genome-wide dN/dS values were 0.27 and 0.23 for episode 1a and 1b, respectively (S1 Table). Therefore, as shown in the frequency spectra, the signature of positive selection is weak at the early stage of the epidemic.

The origin of SARS-CoV-2

The estimated mutation rate of SARS-CoV-2 is 2.4×10^{-3}/site/year with 95% highest posterior density (HPD) of $1.5\text{-}3.3 \times 10^{-3}$/site/year. The mutation rate at the third codon position is 2.9×10^{-3}/site/year (95% HPD $1.8-4.0 \times 10^{-3}$/site/year), which is in a good agreement with synonymous mutation rate of SARS-CoV, $1.67-4.67 \times 10^{-3}$ /site/year [24]. SARS-CoV-2 is estimated to have originated on 12/11/2019 (95% HPD 11/13/2019−12/23/2019). We have to point out that the TMRCA estimation is strongly influenced by the genome sampling scheme. Since the earliest available genome was sampled on 12/24/2019 almost one month after the outbreak, the real origin of the current outbreak may actually be earlier than our estimation.

We estimated genetic variation, including the number of segregating sites, Watterson's estimator of θ, and nucleotide diversity (π) of the SARS-CoV-2. Since both π and θ are estimators of 4Nu (N and u are the effective population size and mutation rate, respectively), they should be close to each other at the mutation-drift equilibrium [25]. Because θ is strongly influenced by rare mutations which are common during recent population expansion [14], it is a better estimator of genetic diversity for SARS-CoV-2. For example, when all samples are considered, θ (13.92×10^{-4}) is approximately eight times higher than π (1.81×10^{-4}, Table 4). Among samples collected from different locations,

sequences from China exhibited higher genetic variation in terms of the number of segregating sites, θ and π, than the rest of the world combined, consistent with the observation that the outbreak originated in China, as the source populations are expected to exhibit higher genetic variation than derived populations [25].

The haplotype network also supports this notion (Fig. 2). Usually, ancestral haplotypes have a greater probability of being in the interior, have more mutational connections, and are geographically more widely distributed. The H1 haplotype is at the center of the network and is found in four countries and many places in China. In addition, a large portion of haplotypes is directly connected to H1. Therefore, it is likely that H1 is the ancestral haplotype. As 45% of H1 are found in Wuhan, this location is the most plausible origin of the ongoing pandemic.

DISCUSSION

A close relationship between SARS-CoV-2 and pangolin_2019 at the amino acid level in the RBD region of the spike protein might be due to recent recombination [15, 16], data contamination, or convergent evolution. Since recent recombination and DNA contamination should affect synonymous and nonsynonymous sites equally, they can be convincingly rejected as great divergence at synonymous sites was observed in spite of similar amino acid sequences between the two genomes. While genotypic convergence may be observed in viruses repeatedly evolving under particular conditions, such as drug resistance and immune escape [26-29], it is otherwise rare. For adaptations that do not involve highly specialized conditions, divergent molecular pathways may develop and genotypic convergence would not be expected [30]. For example, SARS-CoV and SARS-CoV-2 both use the spike protein to bind human ACE2 [2], but five out of six critical amino acids within the RBD are different between these two viruses [17]. Since the SARS-CoV-2

and pangolin_2019 have diverged at about 47% of synonymous sites and infect different hosts, the idea that they share five out of six critical amino acids within RBD through convergent evolution seems far-fetched.

We therefore hypothesize that, instead of convergent evolution, the similarity of RBD between SARS-CoV-2 and pangolin_2019 was caused by an ancient inter-genomic recombination. Assuming a synonymous substitution rate of 2.9×10^{-3}/site/year, the recombination was estimated to have occurred approximately 40 years ago (95% HPD : 31-69 years; divergence time (t) = divergence (dS)/(substitution rate x 2 x 3), considering dS in RBD is 3-fold of genome average). The amino acids in the RBD region of the two genomes have been maintained by natural selection ever since, while synonymous substitutions have been accumulated. If this is true, SARS-CoV-2 may have circulated cryptically among humans for years before being recently noticed.

The ancient origin of SARS-CoV-2 is supported by its lack of a signature of adaptive evolution as shown by frequency spectra and dN/dS in samples from the recent epidemic. For a recently acquired virus, rapid evolution and a strong signature of positive selection are expected. For example, during its short epidemic in 2002-2003, several rounds of adaptive changes have been documented in SARS-CoV genomes [23, 24]. After adapting to its host, the virus may evolve under purifying or relaxed selection, exactly as we see in SARS-CoV-2. Therefore, it is important to sequence samples from the early outbreak and to examine hospital archives for the trace of SARS-CoV-2 ancestors. This information not only can help us to understand the evolutionary path of this virus but also unravel the critical steps for it to achieve effective spreading in humans.

In addition to the RBD, the SARS-CoV-2 spike protein also contains a small insertion of a polybasic cleavage site which was thought to be unique within the B lineage of

betacoronaviruses [17]. However, a recent analysis of bats collected from Yunnan, China, identified a similar insertion in a sequence, RmYN02, closely related to SARS-CoV-2, providing strong evidence that such seemingly sorcerous site insertions can occur in nature [11]. Both the polybasic cleavage site in RmYN02 and RBD in pangolin_2019 suggest that, like with SARS-CoV [6], all genetic elements required to form SARS-CoV-2 may have existed in the environment. More importantly, they can be brought together by frequent intergenomic recombination (see Result). Nature never runs out of material to create new pathogens. It is not whether but when and where the next epidemic will occur.

There is a heated debate about the evolutionary forces influencing the trajectory of the L84S mutation in orf8 protein (http://virological.org/t/response-to-on-the-origin-and-continuing-evolution-of-sars-cov-2/418). While Tang et al. considered Serine is the ancestral amino acid [13], we present evidence that it is a back mutation. The majority of sequences in Wuhan were sampled before early January 2020 and most genomes carrying 84S were found outside Wuhan after middle to late January 2020. The discrepancy in time and space impedes the effort to resolve the debate. It would require more sequences from the early stage of the epidemic to settle this issue. Regardless of its ancestral or derived status, we hypothesize that 84S may confer some selective advantage. Unless the sampling scheme is deliberately skewed, it is difficult to explain such dramatic frequency gain of 84S, from 0 to ~30% in two weeks. Oddly, its frequency ceased to increase after 1/23/2020, when Wuhan was locked down. This coincidence prompts us to consider the effect of social distancing on virus transmission. Another line of evidence comes from the frequency increase of 215V in orf3 protein. The 215V first appeared on 1/22/2020 and rapidly increased its frequency within two weeks.

Several studies suggested that the orf8 protein may function in viral replication, modulating endoplasmic reticulum stress, inducing apoptosis, and inhibiting interferon

300 responses in host cells (41-45 [31 , 32-35]. During the SARS spread, frequency of several
301 orf8 mutations fluctuated in accordance with different phases of the outbreak, suggesting that
302 orf8 underwent adaptation during the SARS epidemic [24]. It is suggested that 84S may
303 induce structural disorder in the C-terminus of the protein and may generate a novel
304 phosphorylation target for Serine/Threonine kinases of the mammalian hosts [36].

305 SARS-CoV orf3 protein has been shown to activate NF-κB and the NLRP3
306 inflammasome and causes necrotic cell death, lysosomal damage, and caspase-1 activation.
307 In addition, orf3 is required for maximal SARS-CoV replication and virulence. All of the
308 above likely contributes to the clinical manifestations of SARS-CoV infection [37-39].
309 Therefore, these two mutations may have some functional consequences and be worth
310 investigating further. By the time we prepared this manuscript, the 215V frequency ceased to
311 increase. However, a parallel mutation has occurred in a different genomic background,
312 further supporting the idea that this mutation may require further study.

313 **MATERIALS AND METHODS**

314 Data collection

315 137 complete SARS-CoV-2 genomes were downloaded from the Global Initiative on
316 Sharing Avian Influenza Data (GISAID, https://www.gisaid.org/). Related coronavirus
317 sequences, including those from five related bat sequences (RaTG13, HUK3-1, ZC45, ZXC-
318 21, and GX2013), two pangolins (each from Guangdong (pangolin_2019) and Guangxi
319 (pangolin_2017)), were downloaded from GenBank
320 (https://www.ncbi.nlm.nih.gov/nucleotide/). Nucleotide positions and coding sequences
321 (CDSs) of SARS-CoV-2 were anchored to the reference genome NC_045512. CDS
322 annotations of other coronaviruses were downloaded from GenBank.

323 Sequence analyses and phylogeny construction

324 CDSs were aligned based on translated amino acid sequences using MUSCLE v3.8.31
325 [40], and back-translated to their corresponding DNA sequences using TRANALIGN
326 software from the EMBOSS package (http://emboss.open-bio.org/) [41]. Nucleotide diversity,
327 including number of segregating sites, Watterson's estimator of θ [42], and nucleotide
328 diversity (π)[43], was estimated using MEGA-X [44]. MEGA-X was also used for
329 phylogenetic construction. Phylogenetic relationships were constructed using the neighbor-
330 joining method based on Kimura's two-parameter model. Number of nonsynonymous
331 changes per nonsynonymous site (dN) and synonymous changes per synonymous site (dS)
332 among genomes were estimated based Li-Wu-Luo's method [45] implemented in MEGA-X
333 and PAML 4 [46].The RDP file for the haplotype network analyses was generated using
334 DnaSP 6.0 [47] and input into Network 10 (https://www.fluxus-engineering.com/) to
335 construct the haplotype network using the median joining algorithm. Four haplotype test
336 implemented in DnaSp was applied to test for possible recombination event.

337 The mutation rate of SARS-CoV-2 and the time to the most recent common ancestor
338 (TMRCA) of virus isolates were estimated by an established Bayesian MCMC approach
339 implemented in BEAST version 1.10.4 [48]. The sampling dates were incorporated into
340 TMRCA estimation. The analysis was performed using the HKY model of nucleotide
341 substitution assuming an uncorrelated lognormal molecular clock [49]. We linked
342 substitution rates for the first and second codon positions and allowed independent rates in
343 the third codon position. We performed two independent runs with 3×10^8 MCMC steps and
344 the results were combined. Log files were checked using Tracer
345 (http://beast.bgio.ed.ac.uk/Tracer). Effective sample sizes were >300 for all parameters.

346

Acknowledgments

The authors thank those who contributed to sequence generation and sharing (The detail is listed in S2 Table). We also thank Chung-I Wu and Wen-Ya Ko for their constructive comments and suggestions. This work was supported by Ministry of Science and Technology, National Taiwan University, and National Taiwan University, College of Medicine, Taipei, Taiwan to HYW (105-2628-B-002-015-MY3, 107-2321-B-002-004-, NTU-109L7806, NSC-131-5), and partially by a grant form Biodiversity Research Center, Academia Sinica to SMC.

References

1. Ren LL, Wang YM, Wu ZQ, Xiang ZC, Guo L, Xu T, et al. Identification of a novel coronavirus causing severe pneumonia in human: a descriptive study. Chin Med J (Engl). 2020. Epub 2020/02/01. doi: 10.1097/CM9.0000000000000722. PubMed PMID: 32004165.
2. Zhou P, Yang XL, Wang XG, Hu B, Zhang L, Zhang W, et al. A pneumonia outbreak associated with a new coronavirus of probable bat origin. Nature. 2020;579(7798):270-3. Epub 2020/02/06. doi: 10.1038/s41586-020-2012-7. PubMed PMID: 32015507.
3. Wu F, Zhao S, Yu B, Chen YM, Wang W, Song ZG, et al. A new coronavirus associated with human respiratory disease in China. Nature. 2020;579(7798):265-9. Epub 2020/02/06. doi: 10.1038/s41586-020-2008-3. PubMed PMID: 32015508.
4. Coronaviridae Study Group of the International Committee on Taxonomy of V. The species Severe acute respiratory syndrome-related coronavirus: classifying 2019-nCoV and naming it SARS-CoV-2. Nat Microbiol. 2020. Epub 2020/03/04. doi: 10.1038/s41564-020-0695-z. PubMed PMID: 32123347.
5. Corman VM, Muth D, Niemeyer D, Drosten C. Hosts and Sources of Endemic Human Coronaviruses. Adv Virus Res. 2018;100:163-88. Epub 2018/03/20. doi: 10.1016/bs.aivir.2018.01.001. PubMed PMID: 29551135.
6. Cui J, Li F, Shi ZL. Origin and evolution of pathogenic coronaviruses. Nat Rev Microbiol. 2019;17(3):181-92. Epub 2018/12/12. doi: 10.1038/s41579-018-0118-9. PubMed PMID: 30531947.
7. Benvenuto D, Giovanetti M, Ciccozzi A, Spoto S, Angeletti S, Ciccozzi M. The 2019-new coronavirus epidemic: Evidence for virus evolution. J Med Virol. 2020;92(4):455-9. Epub 2020/01/30. doi: 10.1002/jmv.25688. PubMed PMID: 31994738.
8. Wu A, Peng Y, Huang B, Ding X, Wang X, Niu P, et al. Genome Composition and Divergence of the Novel Coronavirus (2019-nCoV) Originating in China. Cell Host Microbe. 2020;27(3):325-8. Epub 2020/02/09. doi: 10.1016/j.chom.2020.02.001. PubMed PMID: 32035028.
9. Lu R, Zhao X, Li J, Niu P, Yang B, Wu H, et al. Genomic characterisation and epidemiology of 2019 novel coronavirus: implications for virus origins and receptor binding. Lancet. 2020;395(10224):565-74. Epub 2020/02/03. doi: 10.1016/S0140-6736(20)30251-8. PubMed PMID: 32007145.
10. Chan JF, Kok KH, Zhu Z, Chu H, To KK, Yuan S, et al. Genomic characterization of the 2019 novel human-pathogenic coronavirus isolated from a patient with atypical pneumonia after visiting

386 Wuhan. Emerg Microbes Infect. 2020;9(1):221-36. Epub 2020/01/29. doi:
387 10.1080/22221751.2020.1719902. PubMed PMID: 31987001.
388 11. Zhou H, Chen X, Hu T, Li J, Song H, Liu Y, et al. A novel bat coronavirus reveals natural
389 insertions at the S1/S2 cleavage site of the Spike protein and a possible recombinant origin of HCoV-
390 19. bioRxiv. 2020:2020.03.02.974139. doi: 10.1101/2020.03.02.974139.
391 12. Wu C-I, Poo M-m. Moral imperative for the immediate release of 2019-nCoV sequence data.
392 National Science Review. 2020. doi: 10.1093/nsr/nwaa030.
393 13. Tang X, Wu C, Li X, Song Y, Yao X, Wu X, et al. On the origin and continuing evolution of
394 SARS-CoV-2. National Science Review. 2020. doi: 10.1093/nsr/nwaa036.
395 14. Li W-H. Molecular evolution. Sunderland, Mass.: Sinauer Associates; 1997. xv, 487 p. p.
396 15. Wong MC, Javornik Cregeen SJ, Ajami NJ, Petrosino JF. Evidence of recombination in
397 coronaviruses implicating pangolin origins of nCoV-2019. bioRxiv. 2020:2020.02.07.939207. doi:
398 10.1101/2020.02.07.939207.
399 16. Xiao K, Zhai J, Feng Y, Zhou N, Zhang X, Zou J-J, et al. Isolation and Characterization of 2019-
400 nCoV-like Coronavirus from Malayan Pangolins. bioRxiv. 2020:2020.02.17.951335. doi:
401 10.1101/2020.02.17.951335.
402 17. Andersen KG, Rambaut A, Lipkin WI, Holmes EC, Garry RF. The proximal origin of SARS-CoV-2.
403 Nature Medicine. 2020. doi: 10.1038/s41591-020-0820-9.
404 18. Lam TT-Y, Shum MH-H, Zhu H-C, Tong Y-G, Ni X-B, Liao Y-S, et al. Identification of 2019-nCoV
405 related coronaviruses in Malayan pangolins in southern China. bioRxiv. 2020:2020.02.13.945485. doi:
406 10.1101/2020.02.13.945485.
407 19. Zhang C, Wang M. Origin time and epidemic dynamics of the 2019 novel coronavirus. bioRxiv.
408 2020:2020.01.25.919688. doi: 10.1101/2020.01.25.919688.
409 20. Fay JC, Wu CI. Hitchhiking under positive Darwinian selection. Genetics. 2000;155(3):1405-
410 13. Epub 2000/07/06. PubMed PMID: 10880498; PubMed Central PMCID: PMCPMC1461156.
411 21. Zeng K, Shi S, Wu CI. Compound tests for the detection of hitchhiking under positive
412 selection. Mol Biol Evol. 2007;24(8):1898-908. Epub 2007/06/15. doi: 10.1093/molbev/msm119.
413 PubMed PMID: 17557886.
414 22. Wang HY, Chien HC, Osada N, Hashimoto K, Sugano S, Gojobori T, et al. Rate of evolution in
415 brain-expressed genes in humans and other primates. PLoS Biol. 2007;5(2):e13. Epub 2006/12/30.
416 doi: 10.1371/journal.pbio.0050013. PubMed PMID: 17194215; PubMed Central PMCID:
417 PMCPMC1717015.
418 23. Yeh SH, Wang HY, Tsai CY, Kao CL, Yang JY, Liu HW, et al. Characterization of severe acute
419 respiratory syndrome coronavirus genomes in Taiwan: molecular epidemiology and genome
420 evolution. Proc Natl Acad Sci U S A. 2004;101(8):2542-7. Epub 2004/02/26. doi:
421 10.1073/pnas.0307904100. PubMed PMID: 14983045; PubMed Central PMCID: PMCPMC356986.
422 24. Chinese SMEC. Molecular evolution of the SARS coronavirus during the course of the SARS
423 epidemic in China. Science. 2004;303(5664):1666-9. Epub 2004/01/31. doi:
424 10.1126/science.1092002. PubMed PMID: 14752165.
425 25. Hahn MW. Molecular population genetics. New York, Sunderland, MA: Oxford University
426 Press ; Sinauer Associates; 2018. xviii, 334 pages p.
427 26. Wang HY, Chien MH, Huang HP, Chang HC, Wu CC, Chen PJ, et al. Distinct hepatitis B virus
428 dynamics in the immunotolerant and early immunoclearance phases. J Virol. 2010;84(7):3454-63.
429 Epub 2010/01/22. doi: 10.1128/JVI.02164-09. PubMed PMID: 20089644; PubMed Central PMCID:
430 PMCPMC2838120.
431 27. Xiang D, Shen X, Pu Z, Irwin DM, Liao M, Shen Y. Convergent Evolution of Human-Isolated
432 H7N9 Avian Influenza A Viruses. J Infect Dis. 2018;217(11):1699-707. Epub 2018/02/14. doi:
433 10.1093/infdis/jiy082. PubMed PMID: 29438519.
434 28. Clavel F, Hance AJ. HIV drug resistance. N Engl J Med. 2004;350(10):1023-35. Epub
435 2004/03/05. doi: 10.1056/NEJMra025195. PubMed PMID: 14999114.

29. Locarnini S, Zoulim F. Molecular genetics of HBV infection. Antivir Ther. 2010;15 Suppl 3:3-14. Epub 2010/11/10. doi: 10.3851/IMP1619. PubMed PMID: 21041899.
30. Wen H, Wang HY, He X, Wu CI. On the low reproducibility of cancer studies. Natl Sci Rev. 2018;5(5):619-24. Epub 2019/07/02. doi: 10.1093/nsr/nwy021. PubMed PMID: 31258951; PubMed Central PMCID: PMCPMC6599599.
31. Muth D, Corman VM, Roth H, Binger T, Dijkman R, Gottula LT, et al. Attenuation of replication by a 29 nucleotide deletion in SARS-coronavirus acquired during the early stages of human-to-human transmission. Sci Rep. 2018;8(1):15177. Epub 2018/10/13. doi: 10.1038/s41598-018-33487-8. PubMed PMID: 30310104; PubMed Central PMCID: PMCPMC6181990.
32. Sung SC, Chao CY, Jeng KS, Yang JY, Lai MMC. The 8ab protein of SARS-CoV is a luminal ER membrane-associated protein and induces the activation of ATF6. Virology. 2009;387(2):402-13. doi: 10.1016/j.virol.2009.02.021. PubMed PMID: WOS:000265663100019.
33. Wong HH, Fung TS, Fang S, Huang M, Le MT, Liu DX. Accessory proteins 8b and 8ab of severe acute respiratory syndrome coronavirus suppress the interferon signaling pathway by mediating ubiquitin-dependent rapid degradation of interferon regulatory factor 3. Virology. 2018;515:165-75. Epub 2018/01/03. doi: 10.1016/j.virol.2017.12.028. PubMed PMID: 29294448.
34. Le TM, Wong HH, Tay FP, Fang S, Keng CT, Tan YJ, et al. Expression, post-translational modification and biochemical characterization of proteins encoded by subgenomic mRNA8 of the severe acute respiratory syndrome coronavirus. FEBS J. 2007;274(16):4211-22. Epub 2007/07/25. doi: 10.1111/j.1742-4658.2007.05947.x. PubMed PMID: 17645546.
35. Chen C-Y, Ping Y-H, Lee H-C, Chen K-H, Lee Y-M, Chan Y-J, et al. Open Reading Frame 8a of the Human Severe Acute Respiratory Syndrome Coronavirus Not Only Promotes Viral Replication but Also Induces Apoptosis. The Journal of Infectious Diseases. 2007;196(3):405-15. doi: 10.1086/519166.
36. Ceraolo C, Giorgi FM. Genomic variance of the 2019-nCoV coronavirus. Journal of Medical Virology. 2020;92(5):522-8. doi: 10.1002/jmv.25700.
37. Siu KL, Yuen KS, Castano-Rodriguez C, Ye ZW, Yeung ML, Fung SY, et al. Severe acute respiratory syndrome coronavirus ORF3a protein activates the NLRP3 inflammasome by promoting TRAF3-dependent ubiquitination of ASC. FASEB J. 2019;33(8):8865-77. Epub 2019/04/30. doi: 10.1096/fj.201802418R. PubMed PMID: 31034780; PubMed Central PMCID: PMCPMC6662968.
38. Yue Y, Nabar NR, Shi CS, Kamenyeva O, Xiao X, Hwang IY, et al. SARS-Coronavirus Open Reading Frame-3a drives multimodal necrotic cell death. Cell Death Dis. 2018;9(9):904. Epub 2018/09/07. doi: 10.1038/s41419-018-0917-y. PubMed PMID: 30185776; PubMed Central PMCID: PMCPMC6125346.
39. Castano-Rodriguez C, Honrubia JM, Gutierrez-Alvarez J, DeDiego ML, Nieto-Torres JL, Jimenez-Guardeno JM, et al. Role of Severe Acute Respiratory Syndrome Coronavirus Viroporins E, 3a, and 8a in Replication and Pathogenesis. mBio. 2018;9(3). Epub 2018/05/24. doi: 10.1128/mBio.02325-17. PubMed PMID: 29789363; PubMed Central PMCID: PMCPMC5964350.
40. Edgar RC. MUSCLE: multiple sequence alignment with high accuracy and high throughput. Nucleic Acids Res. 2004;32(5):1792-7. Epub 2004/03/23. doi: 10.1093/nar/gkh340. PubMed PMID: 15034147; PubMed Central PMCID: PMCPMC390337.
41. Rice P, Longden I, Bleasby A. EMBOSS: the European Molecular Biology Open Software Suite. Trends Genet. 2000;16(6):276-7. Epub 2000/05/29. doi: 10.1016/s0168-9525(00)02024-2. PubMed PMID: 10827456.
42. Watterson GA. On the number of segregating sites in genetical models without recombination. Theoretical Population Biology. 1975;7(2):256-76. doi: https://doi.org/10.1016/0040-5809(75)90020-9.
43. Nei M, Li WH. Mathematical model for studying genetic variation in terms of restriction endonucleases. Proc Natl Acad Sci U S A. 1979;76(10):5269-73. Epub 1979/10/01. doi: 10.1073/pnas.76.10.5269. PubMed PMID: 291943; PubMed Central PMCID: PMCPMC413122.

44. Kumar S, Stecher G, Li M, Knyaz C, Tamura K. MEGA X: Molecular Evolutionary Genetics Analysis across Computing Platforms. Mol Biol Evol. 2018;35(6):1547-9. Epub 2018/05/04. doi: 10.1093/molbev/msy096. PubMed PMID: 29722887; PubMed Central PMCID: PMCPMC5967553.

45. Li WH, Wu CI, Luo CC. A new method for estimating synonymous and nonsynonymous rates of nucleotide substitution considering the relative likelihood of nucleotide and codon changes. Mol Biol Evol. 1985;2(2):150-74. Epub 1985/03/01. doi: 10.1093/oxfordjournals.molbev.a040343. PubMed PMID: 3916709.

46. Yang Z. PAML 4: phylogenetic analysis by maximum likelihood. Mol Biol Evol. 2007;24(8):1586-91. Epub 2007/05/08. doi: 10.1093/molbev/msm088. PubMed PMID: 17483113.

47. Rozas J, Ferrer-Mata A, Sanchez-DelBarrio JC, Guirao-Rico S, Librado P, Ramos-Onsins SE, et al. DnaSP 6: DNA Sequence Polymorphism Analysis of Large Data Sets. Mol Biol Evol. 2017;34(12):3299-302. Epub 2017/10/14. doi: 10.1093/molbev/msx248. PubMed PMID: 29029172.

48. Suchard MA, Lemey P, Baele G, Ayres DL, Drummond AJ, Rambaut A. Bayesian phylogenetic and phylodynamic data integration using BEAST 1.10. Virus Evol. 2018;4(1). doi: UNSP vey016

10.1093/ve/vey016. PubMed PMID: WOS:000437019000021.

49. Drummond AJ, Ho SY, Phillips MJ, Rambaut A. Relaxed phylogenetics and dating with confidence. PLoS Biol. 2006;4(5):e88. Epub 2006/05/11. doi: 10.1371/journal.pbio.0040088. PubMed PMID: 16683862; PubMed Central PMCID: PMCPMC1395354.

506 Table 1. Pairwise comparison of nonsynonymous (dN; above slash) and synonymous (dS;
507 below slash) divergence between SARS-CoV-2, RaTG13, and Pangolin_2019 of different
508 coding regions.

Gene	Length (aa)	SARS-CoV-2 vs RaTG13	SARS-CoV-2 vs Pangolin_2019	RaTG13 vs Pangolin_2019
All	9555	0.007/0.168	0.024/0.469	0.025/0.467
		(0.042)*	(0.051)	(0.054)
orf1a	4330	0.008/0.166	0.024/0.472	0.023/0.472
		(0.048)	(0.051)	(0.049)
orf1b	2692	0.003/0.126	0.008/0.505	0.010/0.515
		(0.024)	(0.016)	(0.019)
spike	1219	0.013/0.313	0.068/0.651	0.073/0.680
		(0.040)	(0.104)	(0.107)
RBD of *spike*[A]	219	0.055/0.511	**0.023/0.710**	0.058/0.863
		(0.107)	**(0.032)**	(0.068)
orf3	274	0.009/0.156	0.019/0.285	0.019/0.261
		(0.060)	(0.066)	(0.072)
envelope	75	0/0.018	0/0.037	0/0.018
		(0)	(0)	(0)
matrix	221	0.004/0.186	0.010/0.299	0.006/0.317
		(0.021)	(0.033)	(0.019)
orf6	60	0/0.099	0.014/0.220	0.014/0.345
		(0)	(0.062)	(0.040)
orf7	121	0.011/0.177	0.018/0.275	0.029/0.329
		(0.061)	(0.066)	(0.088)
orf8	121	0.032/0.303	0.025/0.362	0.017/0.391
		(0.105)	(0.069)	(0.042)
nucleocapsid	415	0.005/0.124	0.011/0.145	0.010/0.125

		(0.042)	(0.076)	(0.080)

*Numbers in parentheses are dN/dS

A: RBD, Receptor binding domain of *spike*

509

510

511 Table 2. List of non-singleton mutations of SARS-CoV-2

	Genome position	Gene	RaTG13	Pangolin_2017	Pangolin_2019	Major allele	Minor allele	amount of change		
Nonsynonymous								I	II	
A	614	*orf1ab*	G	G	G	G	A	2		H116Q
B	1190	*orf1ab*	C	C	C	C	T	3		P308S
C	5084	*orf1ab*	A	A	A	A	G	2		A1606T
D	9438	*orf1ab*	C	C	C	C	T	3		T3058I
E	11083	*orf1ab*	G	T	G	G	T	9		L3606F
F	18488	*orf1ab*	T	T	T	T	C	2		I6074V
G	21707	*S*	C	C	N/A	C	T	5		H48Y
H	22661	*S*	G	G	G	G	T	5		V366F
I	26144	*orf3*	G	G	G	G	T	18		G251V
J	27147	*M*	G	G	G	G	C	2		I208T
K	28077	*orf8*	G	G	G	G	C	4		V61L
L	28144	*orf8*	C	C	C	T	C	99	38	L84S
M	28854	*N*	C	C	C	C	T	5		S194L
N	28878	*N*	G	G	G	G	A	6		S202N
O	29019	*N*	A	A	A	A	T	2		D249H
P	29303	*N*	C	C	C	C	T	2		K343I
Synonymous										
α	2662	*orf1ab*	C	T	T	C	T	3		C2397T
β	8782	*orf1ab*	T	T	T	C	T	100	37	C8517T
γ	10138	*orf1ab*	T	T	T	C	T	134	3	C9873T
δ	15324	*orf1ab*	C	C	C	C	T	2		C15059T
ϵ	17373	*orf1ab*	T	C	T	C	T	132	5	C17108T
ζ	18060	*orf1ab*	T	T	A	C	T	131	6	C17795T
η	18603	*orf1ab*	T	T	C	T	A	2		T18338C
θ	23569	*S*	A	C	A	T	C	2		T2007C

ι	23605	*S*	N/A	N/A	N/A	T	G	2		T2043G
κ	24034	*S*	T	C	C	C	T	131	6	C2472T
λ	24325	*S*	A	A	A	A	G	2		A2763G
μ	26729	*M*	T	T	T	T	C	4		T207C
ν	29095	*N*	T	T	T	C	T	125	12	C822T

I Number of changes was inferred by outgroup comparison only

II Number of changes was cross-referenced with the haplotype network of SARS-CoV-2, only numbers which are different from method I are shown.

E: envelope; M: matrix; N: nucleocapsid; S: spike

512

513

514 Table 3. List of dN, dS, and dN/dS in coding regions of SARS-CoV-2 within two episodes

Gene	Episode I (N=57) (2019/12/24-2020/1/21)		Episode II (N=79) (2020/1/22-2020/2/23)		Episode I+II (2019/12/24-2020/2/23)	
	dN X 10^4	dS X 10^4	dN X 10^4	dS X 10^4	dN X 10^4	dS X 10^4
	dN/dS		dN/dS		dN/dS	
All	0.35	1.48	0.79	1.69	0.62	1.61
	0.24		0.47		0.38	
orf1a	0.10	1.27	0.38	1.81	0.27	1.58
	0.08		0.21		0.17	
orf1b	0.06	0.72	0.08	1.46	0.07	1.16
	0.08		0.05		0.06	
spike	0.24	2.29	0.66	1.68	0.49	1.93
	0.1		0.39		0.25	
orf3	0.00	0.00	**5.46**	**(1.69)***	**3.53**	**(1.61)***
	0.00		**3.22**		**2.19**	
envelope	0.00	0.00	0.00	0.00	0.00	0.00
	0.00		0.00		0.00	
matrix	0.00	4.18	1.00	3.07	0.58	3.51
	0.00		0.32		0.17	
orf6	0.00	0.00	0.00	0.00	0.00	0.00
	0.00		0.00		0.00	
orf7	0.00	0.00	0.00	0.00	0.00	0.00
	0.00		0.00		0.00	
orf8	**16.78**	(1.48)*	**16.35**	**(1.69)***	**16.42**	**(1.61)***
	11.32		**9.65**		**10.21**	
nucleocapsid	1.17	6.94	3.02	4.04	2.28	5.34
	0.17		0.75		0.43	

*There were no synonymous mutations in this region. The genome-wide dS value was used

here.

One sequence from South Korea (EPI_ISL_411929) did not have sampling date which was not included in this analysis.

515

516

517 Table 4 Nucleotide diversity of SARS-CoV-2 across geographic regions

Sample origin		Sample size	S	$\theta \times 10^{-4}$	$\pi \times 10^{-4}$
Total		137	223	13.92	1.81
China		64	157	11.38	2.10
	Wuhan	24	41	2.76	1.16
	Rest of China	40	119	9.59	2.62
Rest of the World		73	81	5.71	1.52
	USA	17	28	2.84	1.71
	Rest of the World excluding USA	56	62	4.63	1.43

S: Number of segregating sites.

θ: Nucleotide diversity based on Watterson (*29*)

π: Nucleotide diversity based on Nei and Li (*30*)

518

519

520 **Figure Legend**

521 Figure 1. Frequency spectra of SARS-CoV-2.

522 (A) The direction of changes was based on outgroup comparison with RaTG13. (B) The
523 direction of changes was cross-referenced with the haplotype network showing in Fig. 2

524 Fig. 2 Haplotype network of SARS-CoV-2.

525 Mutation types and numbers are given along the branch. Mutations that are involved in
526 different evolutionary pathways or occurred more than once are enclosed. Also see Table 2
527 for comparison. Six genomes, EPI_ISL_ 408511, 408512, 410480, 408483, 407079, 407079,
528 were excluded from this analysis because they contain too many 'N' in the sequences.

529 Fig. 3 Mutation frequency of 84S is in orf8 and 215V is in orf3.

530 The dashed line indicates the date of the Wuhan, China, lockdown.

531

532 **Appendix Table.**

533 Appendix Table 1. List of dN, dS, and dN/dS in coding regions of SARS-CoV-2 within

534 episode Ia and Ib

Gene	Episode Ia (N=23) (2019/12/24-2020/1/5)		Episode Ib (N=34) (2020/1/6-2020/1/23)	
	dN X 10^4	dS X 10^4	dN X 10^4	dS X 10^4
	dN/dS		dN/dS	
All	0.04	0.13	0.47	2.08
	0.27		0.23	
orf1a	0.00	0.00	0.16	1.58
	0.00		0.10	
orf1b	0.00	0.00	0.09	1.16
	0.00		0.08	
spike	0.00	0.98	0.39	3.09
	0.00		0.13	
orf3	0.00	0.00	0.00	0.00
	0.00		0.00	
envelope	0.00	0.00	0.00	0.00
	0.00		0.00	
matrix	0.00	0.00	0.00	0.00
	0.00		0.00	
orf6	0.00	0.00	0.00	0.00
	0.00		0.00	
orf7	0.00	0.00	0.00	0.00
	0.00		0.00	
orf8	0.00	0.00	**21.31**	**(2.08)***
	0.00		**10.23**	

nucleocapsid	**0.82**	**0.13**	1.43	10.92
	6.35		0.13	

535

536 **Appendix Figures.**

537 **Appendix Figure 1.** The neighbor-joining tree of SARS-CoV-2 related coronaviruses
538 constructed by concatenating coding sequences based on the Kimura 2-parameter model
539 implemented in MEGA-X.

540 **Appendix Figure 2.** Unrooted neighbor-joining tree of SARS-CoV-2 constructed by
541 concatenating coding sequences based on the Kimura 2-parameter model implemented in
542 MEGA-X. Non-singleton changes are shown along the branches.

543 The location of each sequence is given (above the slash) followed by its sampling date
544 (below the slash). For multiple sequences sampled on the same date from the same location,
545 the index, a, b, c, d, and etc. is given. Details are listed in Supplemental File 2.

546 **Appendix Figure 3.** Frequency spectra of SARS-CoV-2 carrying 84L (n=98) (A) and 84S
547 (n=39) (B) in orf8. The direction of changes was cross-referenced with the haplotype network
548 shown in Fig. 2

549

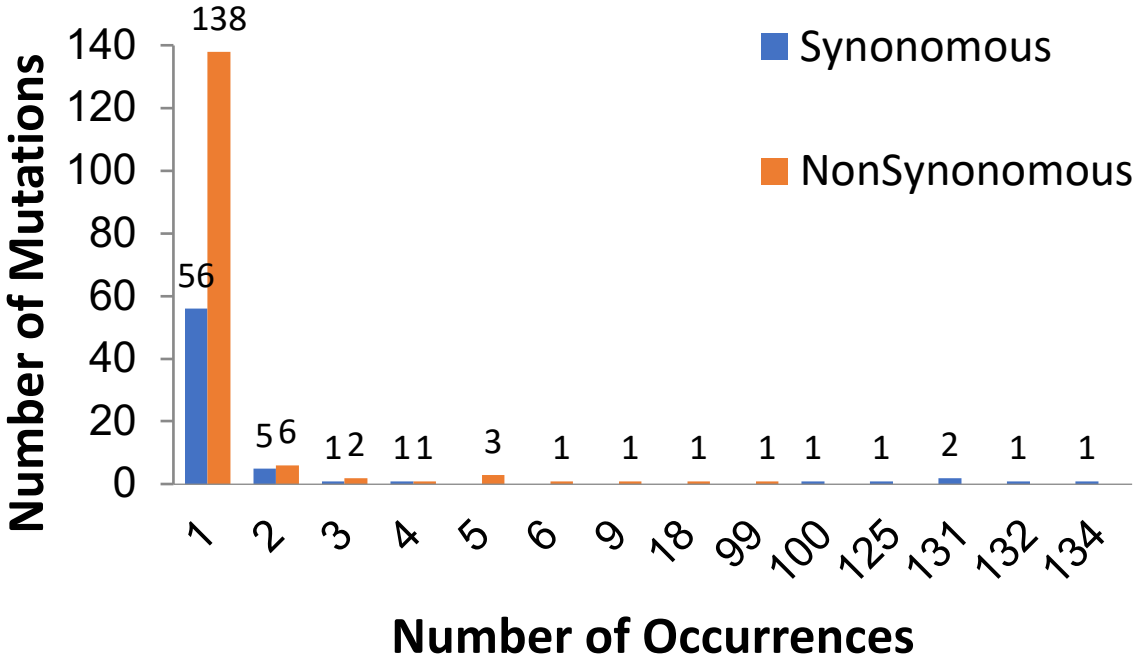

Figure 1. Frequency spectra of SARS-CoV-2.
(A) The direction of changes was based on outgroup comparison with RaTG13.
(B) The direction of changes was cross-referenced with the haplotype network showing in Fig. 2

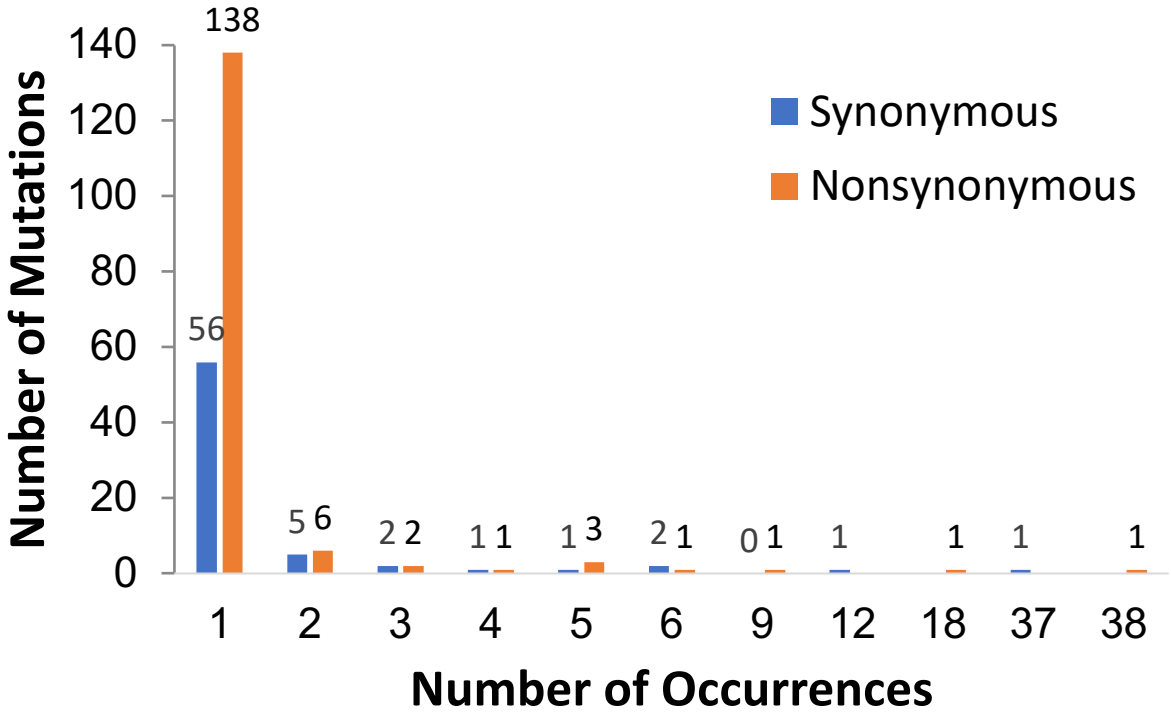

Figure 1. Frequency spectra of SARS-CoV-2.
(A) The direction of changes was based on outgroup comparison with RaTG13.
(B) The direction of changes was cross-referenced with the haplotype network showing in Fig. 2

Geography

Wuhan	USA
Beijing	Taiwan
Chongqing	Singapore
Guangdong	Cambodia
Hangzhou	Japan
Henan	Korea
Guangzhou	Thailand
Hefei	Nepal
Jiangsu	England
Zhejiang	Germany
Foshan	Italy
Fujian	France
Shenzhen	Sweden
Shandong	Belgium
Yunnan	Australia
Sichuan	

NonSynonomous

A	#614	Orf1ab	H116Q
B	#1190	Orf1ab	P308S
C	#5084	Orf1ab	A1606T
D	#9438	Orf1ab	T3058I
E	#11083	Orf1ab	L3606F
F	#18488	Orf1ab	I6074V
G	#21707	S	H48Y
H	#22661	S	V366F
I	#26144	Orf3a	G251V
J	#27147	M	I208T
K	#28077	Orf8	V61L
L	#28144	Orf8	L84S
M	#28854	N	S194L
N	#28878	N	S202N
O	#29019	N	D249H
P	#29303	N	K343I

Synonomous

α	#2662	Orf1ab	C2397T
β	#8782	Orf1ab	C8517T
γ	#10138	Orf1ab	C9873T
δ	#15324	Orf1ab	C15059T
ε	#17373	Orf1ab	C17108T
ζ	#18060	Orf1ab	C17795T
η	#18603	Orf1ab	C18338T
θ	#23569	S	T2007C
ι	#23605	S	T2043G
κ	#24034	S	C2472T
λ	#24325	S	A2763G
μ	#26729	M	T207C
ν	#29095	N	C822T

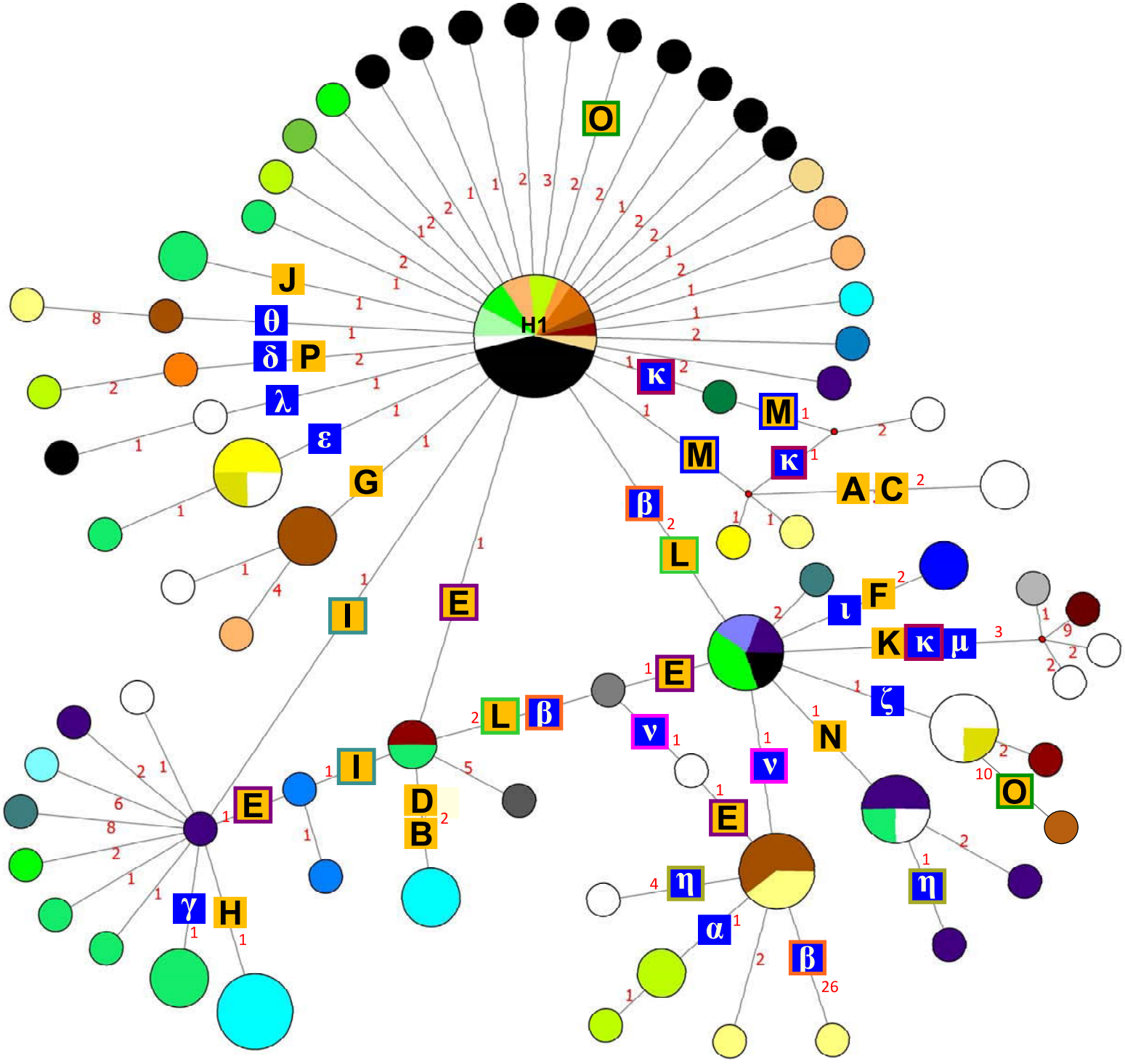

Fig. 2

Fig. 2 Haplotype network of SARS-CoV-2.
Mutation types and numbers are given along the branch. Mutations that are involved in different evolutionary pathways or occurred more than once are enclosed. Also see Table 2 for comparison. Six genomes, EPI_ISL_ 408511, 408512, 410480, 408483, 407079, 407079, were excluded from this analysis because they contain too many 'N' in the sequences.

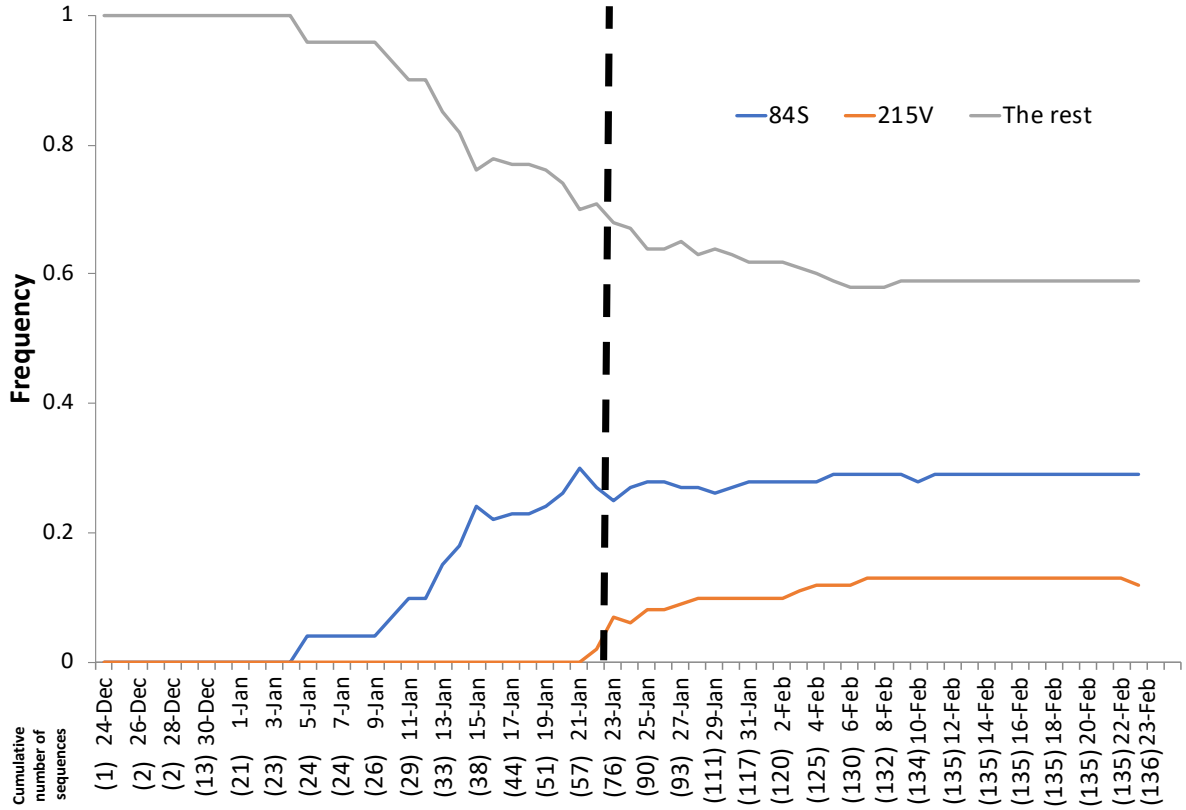

Fig. 3 Mutation frequency of 84S is in orf8 and 215V is in orf3.
The dashed line indicates the date of the Wuhan, China, lockdown.

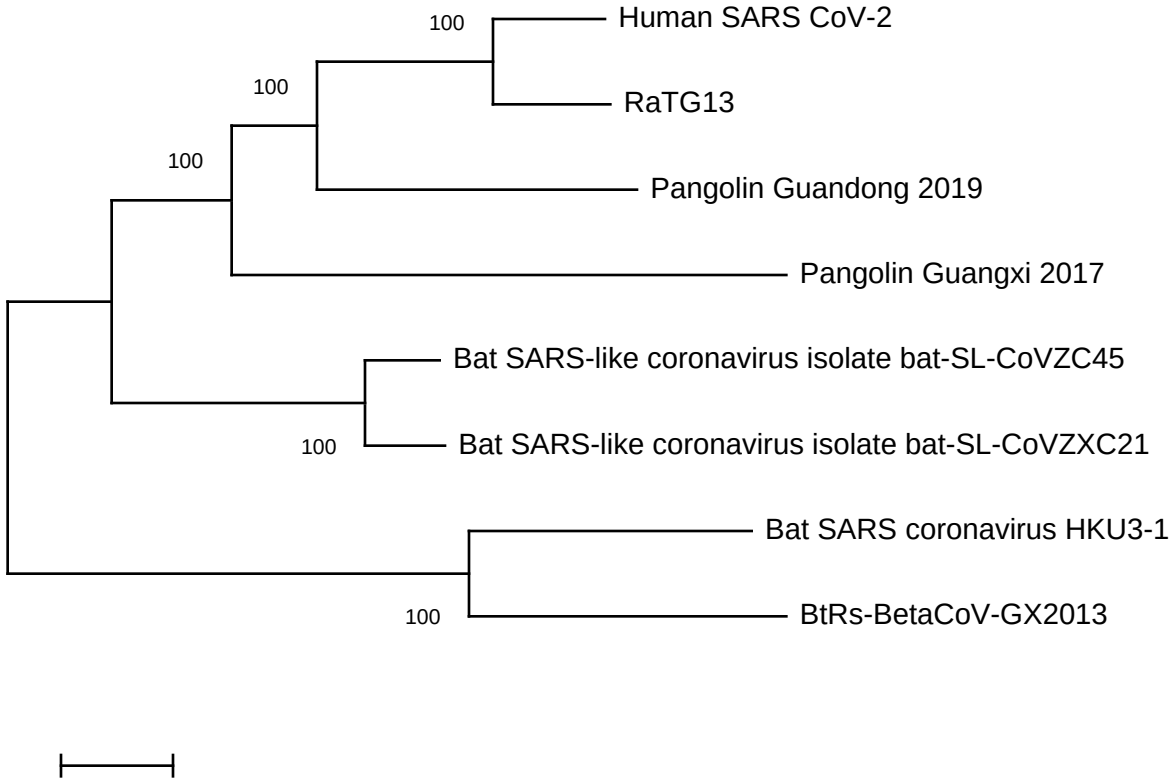

Appendix Figure 1. The neighbor-joining tree of SARS-CoV-2 related coronaviruses constructed by concatenating coding sequences based on the Kimura 2-parameter model implemented in MEGA-X.

NonSynonomous

A	#614	Orf1ab	H116Q
B	#1190	Orf1ab	P308S
C	#5084	Orf1ab	A1606T
D	#9438	Orf1ab	T3058I
E	#11083	Orf1ab	L3606F
F	#18488	Orf1ab	I6074V
G	#21707	S	H48Y
H	#22661	S	V366F
I	#26144	Orf3a	G251V
J	#27147	M	I208T
K	#28077	Orf8	V61L
L	#28144	Orf8	L84S
M*	#28854	N	S194L
N	#28878	N	S202N
O	#29019	N	D249H
P	#29303	N	K343I

* Not Including Nepal/0113

Synonomous

α	#2662	Orf1ab	C2397T
β	#8782	Orf1ab	C8517T
γ	#10138	Orf1ab	C9873T
δ	#15324	Orf1ab	C15059T
ε	#17373	Orf1ab	C17108T
ζ	#18060	Orf1ab	C17795T
η	#18603	Orf1ab	C18338T
θ	#23569	S	T2007C
ι	#23605	S	T2043G
κ	#24034	S	C2472T
λ	#24325	S	A2763G
μ	#26729	M	T207C
ν	#29095	N	C822T

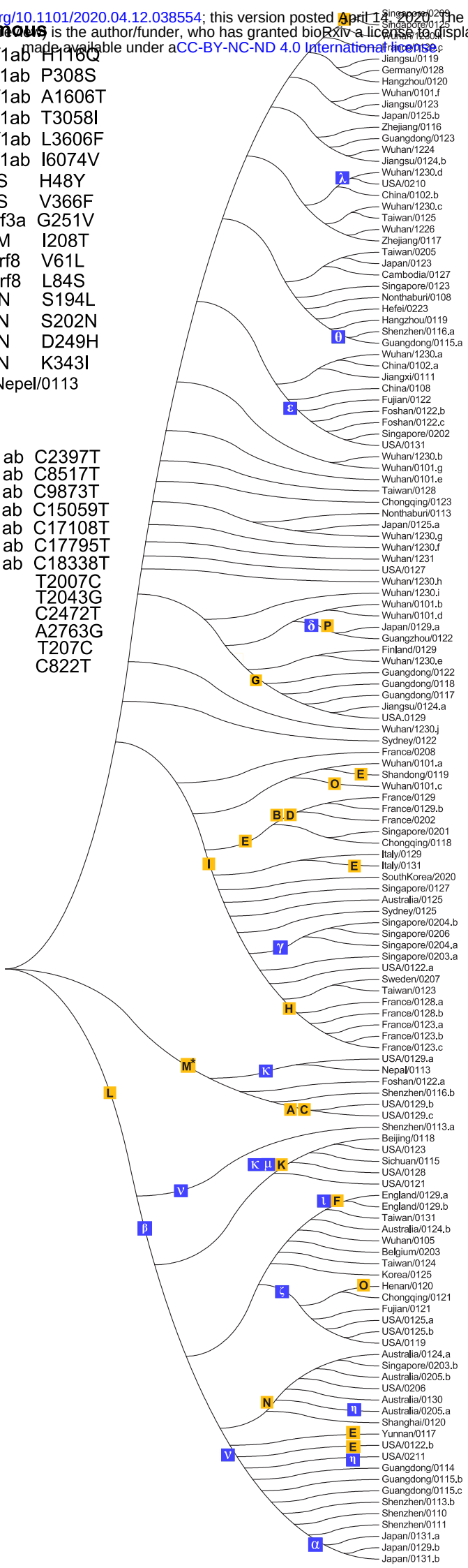

Appendix Figure 2. Unrooted neighbor-joining tree of SARS-CoV-2 constructed by concatenating coding sequences based on the Kimura 2-parameter model implemented in MEGA-X. Non-singleton changes are shown along the branches.

The location of each sequence is given (above the slash) followed by its sampling date (below the slash). For multiple sequences sampled on the same date from the same location, the index, a, b, c, d, and etc. is given. Details are listed in Supplemental File 2.

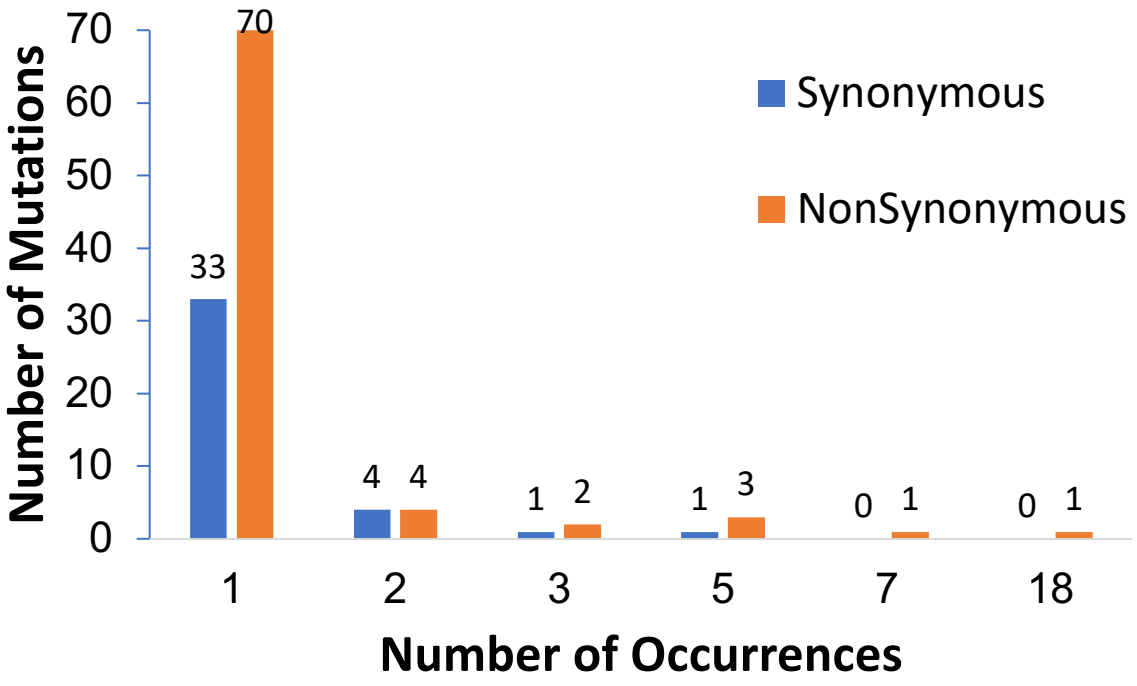

Appendix Figure 3. Frequency spectra of SARS-CoV-2 carrying 84L (n=98) (A) and 84S (n=39) (B) in orf8. The direction of changes was cross-referenced with the haplotype network shown in Fig. 2

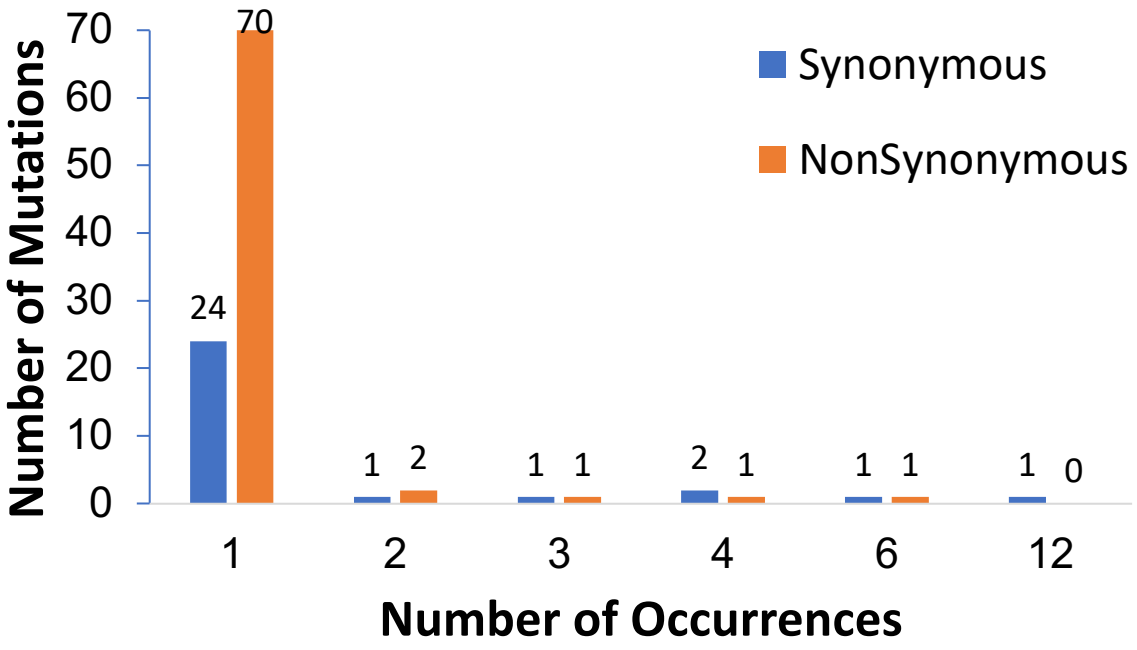

Appendix Figure 3. Frequency spectra of SARS-CoV-2 carrying 84L (n=98) (A) and 84S (n=39) (B) in orf8. The direction of changes was cross-referenced with the haplotype network shown in Fig. 2